NASA TT F-9319

NASA TT F-9319

EXPERIENCE GAINED IN USE OF AN ELECTROSTATIC ANALYZER ON BOARD THE "KOSMOS-12" SATELLITE

V.V.Mel'nikov, I.A.Savenko, B.I.Savin,
and P.I.Shavrin

Translation of "Opyt primeneniya elektrostaticheskogo analizatora na sputnike 'Kocmoc-12'".
Geomagnetizm i Aeronomiya, Vol.5, No.1, pp.148-154, 1965

NATIONAL AERONAUTICS AND SPACE ADMINISTRATION
WASHINGTON APRIL 1965

NASA TT F-9319

EXPERIENCE GAINED IN USE OF AN ELECTROSTATIC ANALYZER ON BOARD THE "KOSMOS-12" SATELLITE */148

V.V.Mel'nikov, I.A.Savenko, B.I.Savin, and P.I.Shavrin

21630

The article describes the design of a spherical electrostatic analyzer, used for investigating fluxes of electrons and positive ions with an energy E = 1 Kev during the flights of the Kosmos-12 and Kosmos-15 satellites. The operating characteristics of the analyzer were as follows: transmission bandwidth $\Delta E/E \sim 30\%$ and sensitivity threshold (assuming flux isotropy) $\sim 6 \times 10^6$ particles/cm^2 sec Kev. The results of measurements during the flight of Kosmos-12 are presented. The constantly present electron and ion fluxes with E = = 1 Kev on the night side of Earth usually do not exceed the sensitivity threshold of the instrument. South of New Zealand, instances of increase in the intensity of, chiefly, electrons with E = 0.5 - 1 Kev have been observed. The appearance of electrons and ions with E = 1 Kev over the Pacific has been recorded. Author

Below is described an electrostatic spherical analyzer (Bibl.1, 2) for the investigation of fluxes of electrons and positive ions with E = 1 Kev. Analyzers of this kind were installed on board the satellites Kosmos-12 and Kosmos-15. The launching date of the satellites and their orbit parameters are

* Numbers in the margin indicate pagination in the original foreign text.

given in the Table.

Satellite	Launching date	Apogee, km	Perigee, km	Period, min.	Angle of Inclination of Orbital Plane
«Kosmos-12»	22 Dec. 1962	405	211	90.45	65°
«Kosmos-15»	22 Apr. 1963	371	173	89.77	65°

The method of measuring the weak currents generated by the recorded electron or ion fluxes has been described elsewhere (Bibl.2). The American investigators used electrostatic analyzers in the Explorer XII satellite (Bibl.3) and Mariner II space probe (Bibl.4).

Apparatus. Properly speaking, the analyzer was a spherical capacitor (Fig.1) with symmetric potentials -U/2 and +U/2 fed to its plates. The charged particles incident on the gap between the plates were deflected by an electric field and entered a Faraday cylinder at the analyzer output.

The deflection angle of the trajectory of a particle traveling along zero equipotential within the gap is 120°, neglecting the additional deflection in the scattered field at the inlet and outlet of the gap, which is no more than 2.5°.

The outer-surface radius of the working gap is 66 mm and the inner-surface radius, 54 mm. The plates of the spherical capacitor are of copper and were especially machined to reduce the proportion of charged particles elastically rebounding from the sphere surfaces. The machined surfaces were subsequently silver-plated to reduce light reflection in the ultraviolet region of the spectrum (Bibl.5). The spheres of the analyzer are enclosed in a thin /149
aluminum housing linked to the satellite body. Mounted on the housing is a conical intake diaphragm. The geometry of the inlet and outlet diaphragms of the analyzer was chosen in accordance with calculations of the electron-optical

characteristics of a 120^0 analyzer (Bibl.1). Mounted directly in front of the gap inlet and beyond the gap outlet are cone-shaped screens attached to the satellite body; their purpose is to reduce the effect of the scattered fields.

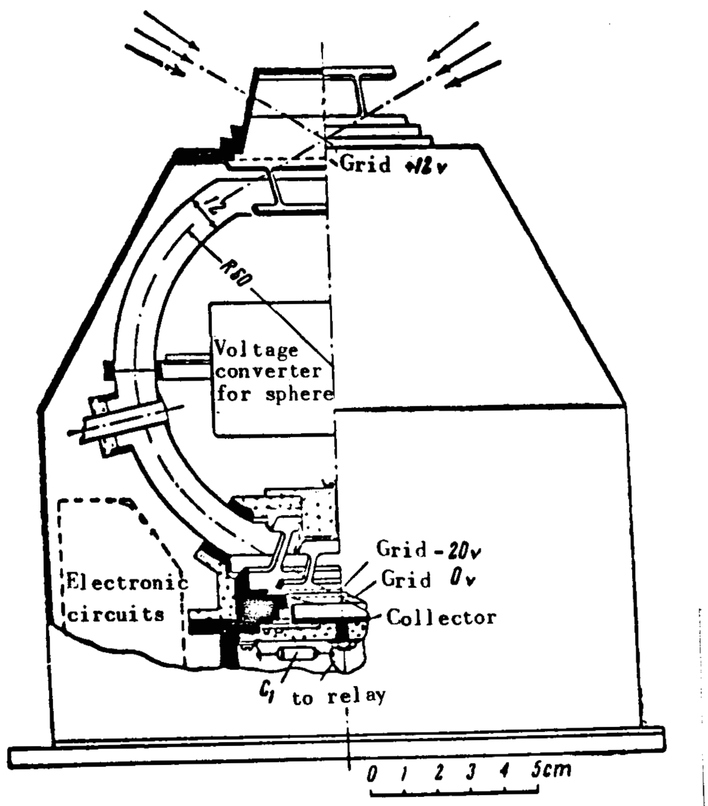

Fig.1

If a charged particle flux with directional intensity i(E) particles/cm^2 sec ster Kev exists in the space outside the analyzer, the flux emerging from the analyzer will be

$$N = \int_{E_0-\Delta E/2}^{E_0+\Delta E/2} i(E)L(E)dE \text{ prtls/sec.}$$

where L(E) is the transmission through the analyzer; $E_0 - \Delta E/2$ and $E_0 + \Delta E/2$ are the edges of the transmission band. To assess the geometric factor G of the analyzer, we represent the shape of the line L(E) of the analyzer in the form of a triangle with the height $L(E_0) = L_0$ and the base ΔE. Further, we replace $i(E)$ by $\bar{i}(E_0)$. Then,

$$N \simeq \bar{i}(E_0) \int_{E_0-\Delta E/2}^{E_0+\Delta E/2} L(E)\,dE = \bar{i}(E_0) L_0 \frac{\Delta E}{2} = \bar{i}(E_0) L_0 \frac{\Delta E}{E_0}\frac{E_0}{2} = \bar{i}(E_0) G.$$

whence

$$G = \frac{1}{2} L_0 \left(\frac{\Delta E}{E_0}\right) E_0 \ cm^2 \ ster \ kev.$$

Mel'nikov et al (Bibl.1) calculated that, for this analyzer, disre- /150
garding the shadowing effect of the outlet diaphragms, $L_0 = 0.066\ r_0^2$ cm^2 ster, where r_0 is the radius of the mean equipotential in the gap. This value of L_0 is the maximum possible ($L_{0\,max}$) for the analyzer considered here; $L_{0\,max} = 2.4$ cm^2 ster for $r_0 = 6$ cm. The maximum relative transmission bandwidth,

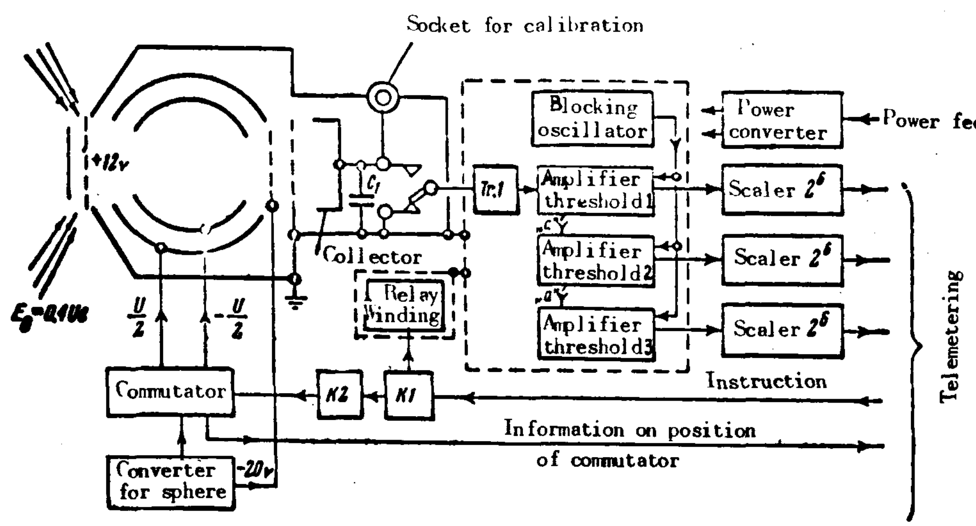

Fig.2

calculated earlier (Bibl.1) and determined solely by the incidence of particles on the surface of the spheres, is $(\Delta E/E_0)_{max} = 6\ a = 0.6$, where $a = \Delta r/2r_0 = 0.1$. The minimum $(\Delta E/E_0)_{min}$, pertaining to the particles that enter the gap at a tangent to the mean equipotential and travel in the meridional plane, is 0.08 for this analyzer (Bibl.1).

For an actual device, allowance must be made for the decrease in the transmission bandwidth $\Delta E/E_0$ and for the luminance L_0 compared with their maximum values, due to the effect of the diaphragms, the finite size of the collector, and the partial shadowing of the collector by the grids, i.e., $L_0 < < L_{0\,max}$ and $(\Delta E/E_0)_{min} < \Delta E/E_0 < (\Delta E/E_0)_{max}$. Assuming $\Delta E/E_0 \sim 0.3$ and $L_0 \sim \sim 0.7$ cm^2/ster, we have $G \sim 0.1\ E_0$ cm^2 ster Kev.

The energy E_0 at the transmission band maximum, for this geometry of a deflecting capacitor, is correlated to the potential difference on the capacitor plates by the expression

$$U(v) = 0.4\,E_0(ev).$$

The plates were fed with potentials from a high-voltage converter located inside the inner sphere, across a high-voltage commutator (Fig.2). The potential difference and its sign were reversed on command from the satellite during the flight. The analyzer installed on board the Kosmos-12 could be adjusted to the registration of electrons with energies of $E_0 = 0.5$ and 1 Kev and of positive ions with $E_0 = 1$ Kev. On Kosmos-15 the analyzer was adjusted to electrons and positive ions with $E_0 = 1$ Kev. Here, in one of the four positions of the commutator, both spheres were linked to the instrument casing. To prevent the incidence of thermal ions of the ionosphere on the working gap, the inlet of the analyzer installed on Kosmos-15 was covered by a grid fed with a potential of +12 v relative to the satellite body.

The particle collector in the analyzer was a Faraday shield (Fig.1) /151 made of duraluminum and attached to an insulator of polished Plexiglas. The inner surface of the Faraday cylinder was finned so as to reduce the yield of secondary electrons. On the bottom side, the collector was surrounded by shielding metal portions of the device. The intake port of the collector was covered by two grids, the nearer grid being attached to the instrument casing and the farther grid being maintained at a -20 v potential relative to the casing in order to suppress secondary electrons and photoelectrons from the Faraday cylinder. These grids also weaken the capacitive coupling between the collector and the spheres on which high voltages are periodically reversed. The stream of particles incident on the collector was measured by means of an electrometric circuit based on the principle of charge accumulation on the capacitor C_1 during the time T and conversion of the value of the accumulated charge to a number of pulses (Bibl.2).

The storage capacitor was represented by polystyrene film capacitors with a capacitance of 100 μμf. The leakage resistance of such capacitors is at least 10^{13} ohms and their absorption factor $\sim 10^{-3}$.

The electrometric circuit made it possible to measure currents beginning with $\sim 8 \times 10^{-15}$ a = 5×10^4 particles/sec = N_{min}. Such a current on the collector corresponded to a minimum total flux intensity of

$$I_{min}(E_0) = 4\pi \bar{i}(E_0) = 4\pi \frac{N_{min}}{G} \approx 6 \cdot 10^6 \frac{1}{E_0} \text{ hrs /cm}^2 \text{ sec kev.}$$

The dynamic range of the circuit was about ~ 1000. The charge accumulation time was T = 120 sec, determined by the repetition rate of instructions from the satellite to the cell K1 (Fig.2). The cell K1 formed a pulse of a duration of ~ 200 msec to close the discharge relay of the storage capacitor. At the trailing edge of this pulse, the cell K2 was triggered in order to, in its turn, form a pulse for triggering the weak-current relay across the contacts from which current was fed to the winding of the high-voltage commutator. The pulse triggering the commutator armature was somewhat delayed in the inductances of the windings of the relay and commutator, so that attraction of the commutator armature set in after the storage capacitor had already discharged and the input of the electrometric circuit had closed with respect to the body. Reversal of the high voltage on the spheres occurred during the return stroke of the commutator armature.

The high-voltage converter, commutator, and electrometric circuit were housed in the outer unit of the device, positioned on the external surface of the satellite (Fig.1). The scaler loop, instruction register, and power converter were placed inside a sealed container. During charge accumulation, information on the states of the flip-flops was telemetered to the ground, together with information on the number of the commutator position. In the presence of current in the collector, the flip-flop states were switched immediately following the passage of a pulse train from the electrometric circuit.

Tuning, calibration of the circuit, and preflight checkups were performed by means of weak current, fed from the control console across a calibration socket (Bibl.2).

Results (Kosmos-12). Preliminary results of measurements by means of analyzers on board the Kosmos-12 and Kosmos-15 were published previously (Bibl.6). Figure 3 gives the plots of readings of the analyzer installed on Kosmos-12 for the period from 22 to 30 December for loops during which information on the analyzer operation was available. The time in units of T - the interval of charge accumulation in the capacitor C_1, is plotted along the horizontal axes. The solid and broken curves in each "stage" of Fig.3 pertain to a single loop. Plotted along the vertical axis, for each loop, is the potential difference for the storage capacitor, in millivolts. The sensitivity threshold of the circuit of about 10 mv corresponds to a total intensity of $I \sim 6 \times 10^6$ particles/cm^2 sec Kev for E_0 = 1 Kev. For orientation, a scale of /152

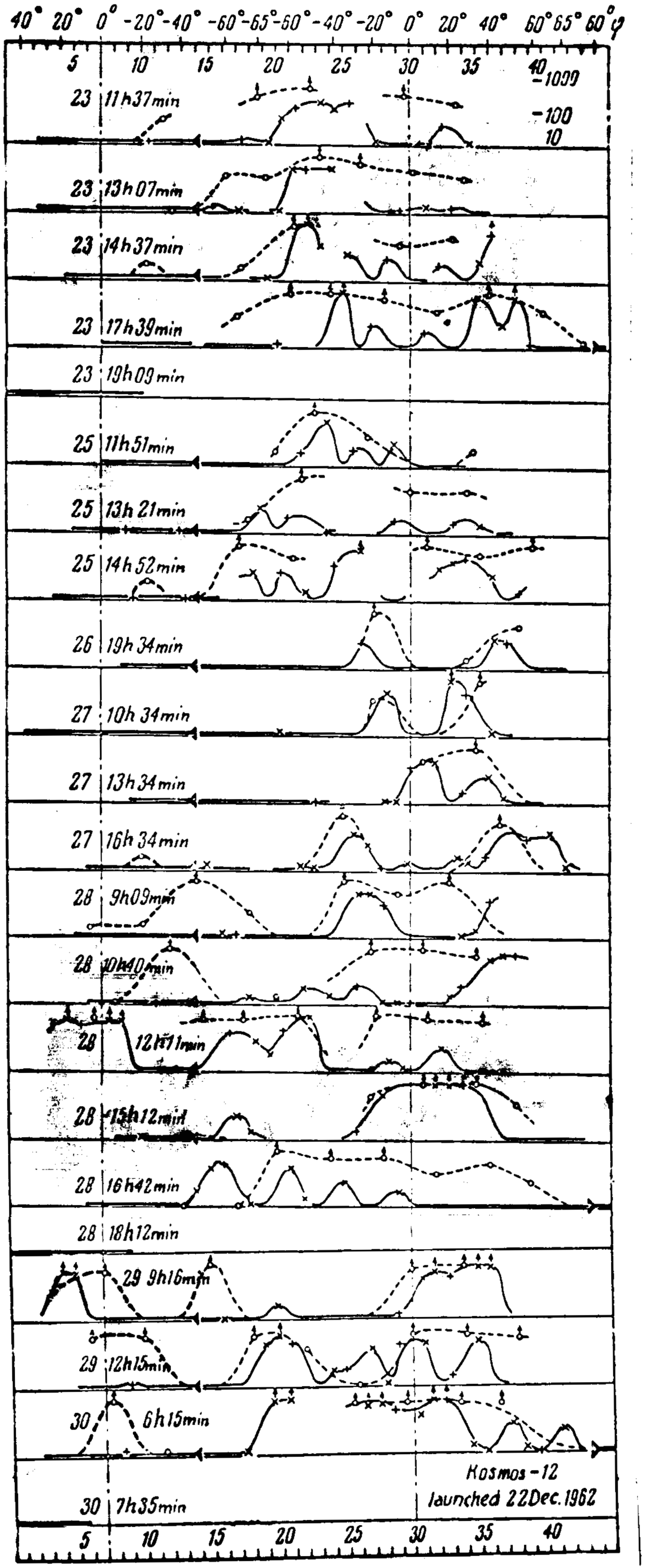
40° 20° 0° -20° -40° -60° -65° -60° -40° -20° 0° 20° 40° 60° 65° 60° φ
5 10 15 20 25 30 35 40
-1000
-100
10
23 11h37min
23 13h07min
23 14h37min
23 17h39min
23 19h09min
25 11h51min
25 13h21min
25 14h52min
26 19h34min
27 10h34min
27 13h34min
27 16h34min
28 9h09min
28 10h40min
28 12h11min
28 15h12min
28 16h42min
28 18h12min
29 9h16min
29 12h15min
30 6h15min
30 7h35min
Kosmos-12
launched 22Dec.1962

Fig.3

geographic latitudes in degrees is entered at the top. At the points of intersection of the horizontal axes with the vertical dot-dash lines, the satellite passes across the equator on the day and night sides of the Earth. The numerals to the left indicate the date and time of transit across the night equator during a given loop. The circles in Fig.3 pertain to the case of absence of a deflecting field in the gap; the straight crosses, to adjustment to positive ions; the oblique crosses, to adjustment to electrons. Since the experimental points are fairly rare, the curves were plotted along them solely with the object of facilitating perception. The heavy solid-line segments of the curves correspond to the stay of the satellite in the Earth's shadow.

To determine the instants of entry of the satellite into the Earth's shadow and emergence therefrom, the trajectory of the satellite was projected in the xy-plane perpendicular to the Earth-Sun axis.

Obviously, two of the four intersections of the orbital projection by the projection of the Earth's surface (disregarding atmospheric refraction) will give the instants of entry of the satellite into the Earth's shadow and its emergence therefrom.

Calculations show that, during the several days of flight of Kosmos-12, the latitude of emergence from the shadow did not vary much and was equal to -46°. Figure 4 shows the geographic position of the night-time segments of the trajectory for the loops already examined in Fig.3. The thin solid lines correspond to the trajectory segments during which information on the analyzer operation was available. The heavy broken and solid lines along the trajectory as well as the numerals have the same meaning as in Fig.3. For the orbital loop No.26 (19h 34m), the daytime segment is shown.

An examination of Figs.3 and 4, along with the inference that the analyzer performed normally, may suggest the following conclusions.

1. Until 28 December on the dark side of the Earth the continuously present intensity of electrons and ions with an energy of ~ 1 Kev was less than 6×10^6 particles/cm^2 sec Kev, assuming the existence of isotropy. During two orbital loops, No.28 (12h 11m) and No.29 (9h 16m), above the equatorial regions of the Pacific, the analyzer recorded an increased ($> 10^8$ particles/cm^2 sec Kev) intensity of electrons and ions with an energy of ~ 1 Kev, which may be associated with the solar flare of point 1 which took place on 24 December.

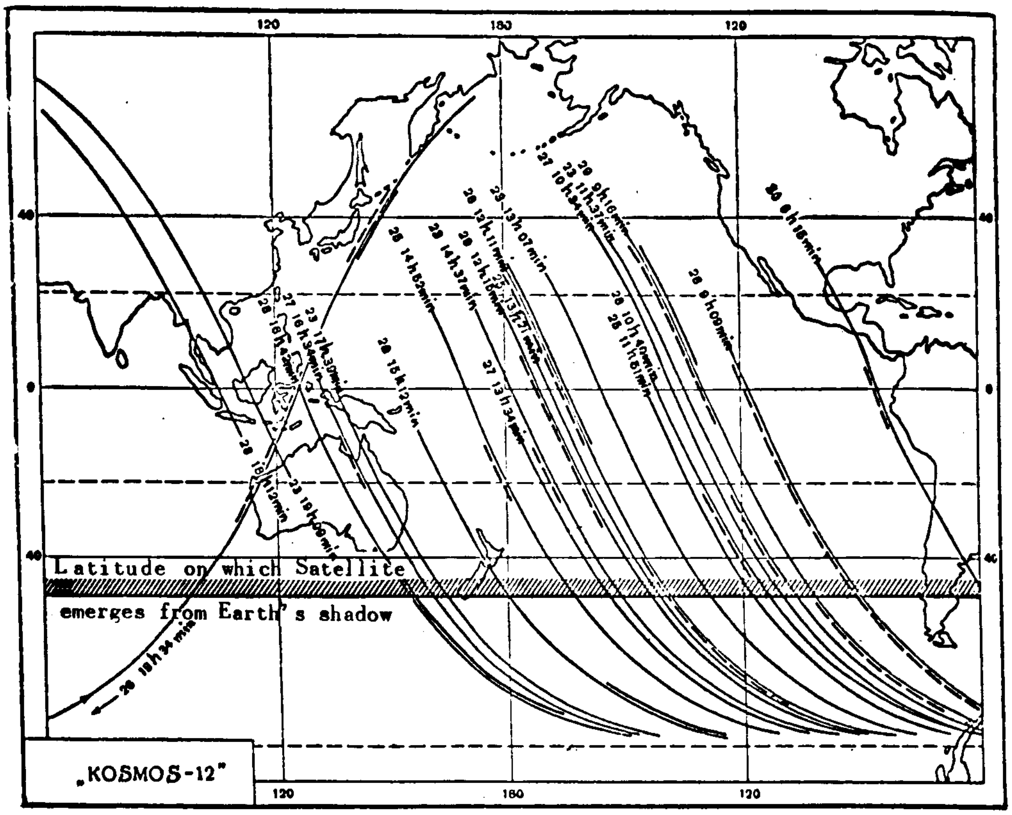

Fig.4

It is also interesting to note the appearance of signals from the analyzer output during the absence of a deflecting field in the gap on the night-time segments of the loops Nos.23 (11h 37m, 13h 07m, 14h 37m), 25 (14h 52m), 27 (16h 34m), 28 (9h 09m, 10h 40m, 15h 12m), 29 (12h 15m) in the neighborhood of values 10 - 15 on the bottom scale in Fig.3. The regions of appearance of these signals cluster around a magnetic envelope with L $\sim$ 1.4, which warrants the assumption that the particles registered in those regions are low-energy particles associated with the existence of the inner radiation belt, which penetrate into the collector after being bounced off the working surfaces of the analyzer. It is difficult, however, to estimate the energy and intensity of these particles. It can only be stated that, if they are electrons, their energy exceeds 20 ev.

2. On the daytime segments of all the loops it was impossible to detect any constant intensity level exceeding 6×10^6 particles/cm^2 sec Kev with respect to electrons and ions with an energy of $\sim$ 1 Kev. Signals of extremely varying magnitude were, however, received from the analyzer each time the /154
satellite passed across the illuminated side of Earth. These signals may have been provoked by photoelectrons from the collector grids (crosses) or by the combined effect of photoelectrons and thermal ions of the ionosphere, which penetrated through the gap between the spheres. The slope of the curves is apparently related to the nature of the roll of the satellite.

3. On the adjacent loop No.28 (15h 12m and 16h 42m) in the region south of New Zealand, instances of increased ($\sim 10^8$ particles/cm^2 sec Kev) intensity of charged particles were recorded. This region was in the vicinity of the southern isochasm.

In conclusion, the authors wish to express their appreciation to V.Ya. Shiryayeva and N.M.Safronova for assistance in constructing the instrument, and also to Yu.V.Trigubov and L.A.Smirnov for adjustment of the analyzer and its preparation for launching.

BIBLIOGRAPHY

1. Mel'nikov, V.V., Savenko, I.A., and Savin, B.I.: Geomagn. i aeronomiya, Vol.1, No.6, p.981, 1961.

2. Goryunov, N.N., Savin, B.I., and Sosnovets, E.N.: Space Research (Kosmicheskiye issledovaniya). 1965 (in print).

3. Bader, M.: I.G.R., Vol.67, No.13, p.5007, 1962.

4. Neugebauer and Snyder: Science, Vol.138, No.3455, p.1095, 1962.

5. Johnson, B.K.: Proc. Phys. Soc., Vol.53, No.3, p.258, 1941.

6. Vernov, S.N., Mel'nikov, V.V., Savenko, I.A., Savin, B.I., and Shavrin, P.I.: Paper presented at the All-Union Conference on Cosmic-Ray Physics. Apatites, 1964.

Moscow State University,
Institute of Nuclear Physics

Submitted: 17 September 1964